



HAL
open science

Real-time control strategies for hybrid vehicles issued from optimization algorithm

Grégory Rousseau, Antonio Sciarretta, Delphine Sinoquet

► To cite this version:

Grégory Rousseau, Antonio Sciarretta, Delphine Sinoquet. Real-time control strategies for hybrid vehicles issued from optimization algorithm. Hybrid and Vehicles Energy Management, Feb 2007, Braunschweig, Germany. hal-02284283

HAL Id: hal-02284283

<https://ifp.hal.science/hal-02284283>

Submitted on 11 Sep 2019

HAL is a multi-disciplinary open access archive for the deposit and dissemination of scientific research documents, whether they are published or not. The documents may come from teaching and research institutions in France or abroad, or from public or private research centers.

L'archive ouverte pluridisciplinaire **HAL**, est destinée au dépôt et à la diffusion de documents scientifiques de niveau recherche, publiés ou non, émanant des établissements d'enseignement et de recherche français ou étrangers, des laboratoires publics ou privés.

REAL-TIME CONTROL STRATEGIES FOR HYBRID VEHICLES ISSUED FROM OPTIMIZATION ALGORITHM

Gregory Rousseau ^{*,**} Antonio Sciarretta ^{*}
Delphine Sinoquet ^{*}

^{*} *Institut Français du Pétrole, 1 et 4, avenue de
Bois-Préau, 92852 Reuil-Malmaison Cedex - France*

^{**} *Ecole des Mines de Paris*

Tel. 0033 1 47 52 63 24 / Fax. 0033 1 47 52 70 12
gregory.rousseau@ifp.fr

Abstract: This paper focuses on a mild-hybrid city car (Smart), equipped with a starter-alternator, where the kinetic energy in the braking phases can be recovered to be stored in a supercapacitor, and re-used later via the electric motor. The additional traction power allows to downsize the engine and still fulfill the power requirements. Moreover, the engine can be turned off in idle phases. The optimal control problem of the energy management between the two power sources is solved for given driving cycles by a classical dynamic programming method. From dynamic models of the electric motor and supercapacitor a quasistatic model of the whole system is derived and used in the optimization. The real time control law to be implemented on the vehicle is derived from the resulting optimal control strategies.

Keywords: Hybrid vehicle, Optimal control, Dynamic programming

1. INTRODUCTION

Growing environmental concerns coupled with concerns about global crude oil supplies stimulate research on new vehicle technologies. Hybrid-Electric Vehicles (HEV) appear to be one of the most promising technologies for reducing fuel consumption and pollutant emissions. HEVs can save fuel thanks to: (i) the possibility of turning off the engine in idle phases (*stop-and-go*), (ii) the recuperation of braking energy to be stored in the battery and re-used later via the electric motor, (iii) the possibility of downsizing the engine, and (iv) the optimization of energy flows.

The energy management of hybrid powertrains requires some specific supervisory control laws. This controller relies on the estimation of the

battery state of charge, and it must take into account the variable efficiency of each element of the powertrain. Optimization of energy-management strategies on prescribed driving cycles (offline optimization) is often used to derive sub-optimal control laws to be implemented on the vehicle (Sciarretta *et al.*, 2004), (Scordia, 2004), (Wu *et al.*, 2002), (Delprat, 2002).

Optimization tools require a mathematical description of the system. In most offline optimization techniques, the quasistatic backward modelling approach is used. On the other hand, dynamic forward-facing models are necessary to accurately simulate the system and to identify the main system parameters.

In this paper, we present a dynamic model of the electric propulsion system of a mild hybrid vehicle. The quasistatic version of the model is used in a Dynamic Programming algorithm to optimize the energy management of the vehicle. Finally, we propose a real-time feedback control strategy derived from the offline optimization results, which is validated for typical driving conditions.

2. SYSTEM MODELLING

IFP, in partnership with Gaz de France and ADEME, has applied its downsizing technology to a natural gas engine, resulting in a small urban demonstrator vehicle (VEHGAN vehicle). The conventional powertrain is integrated with a belt-driven starter–alternator and a supercapacitor, both provided by Valeo (Tilagone and Venturi, 2004).

The resulting architecture is a mild-hybrid powertrain: the torque requested for traction cannot be provided by the electric motor only. Thus, the engine cannot be turned off, except during idling (*stop-and-go*).

In order to optimize the energy management of the VEHGAN, we use either a quasistatic backward model, or a more detailed AMESim model (Dabadie *et al.*, 2005) to calculate the speed $\omega_{rq}(t)$ and torque $T_{rq}(t)$ required at the engine output shaft along a prescribed drive cycle. This torque request can be split between the engine torque $T_e(t)$ and the electric motor torque $T_m(t)$. Finding the optimal splitting strategy is the objective of the supervisory controller. To evaluate the performance of the two components as a function of their respective torque, we build a simplified model of the system, which consists of:

- a model of the 0.660 l natural gas engine; the engine performance is characterized by the fuel consumption map displayed in Figure 1 and by its maximum torque $T_e^{max}(\omega_{rq})$ that depends on the engine speed (see (18)),
- a model of the 3 kW starter alternator (described in section 2.1.1),
- a model of the supercapacitor, which is made up of 12 modules of 1500 F; this model is described in section 2.1.2.

2.1 Submodels of the electric components

2.1.1. Electric motor The starter–alternator used in the VEHGAN vehicle is a permanent-magnet motor with six magnets. A realistic model of torque evolution, as described in (Sciarretta *et al.*, 2004), is given by

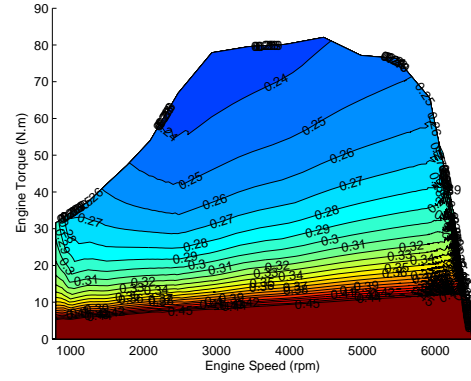


Fig. 1. Fuel consumption map of natural gas engine of VEHGAN vehicle

$$T_m(t) = \frac{3}{2}p\varphi_m \cdot \frac{R_{st}U_q(t) - p\omega(t)R_{st}\varphi_m - p\omega(t)L_{st}U_d(t)}{R_{st}^2 + p^2\omega^2(t)L_{st}^2}, \quad (1)$$

where $\omega(t)$ is the rotor speed, R_{st} the stator resistance, $\varphi_m(t)$ the mutual flux linkage, $U_q(t)$ and $U_d(t)$ are the d-q axis stator voltage components, L_{st} is the stator inductance, and p is the number of pole pairs.

For simplification convenience, we choose to model this motor using DC motor equations by neglecting the non-linear contribution. We then replace (1) by

$$T_m(t) = \frac{1}{R_a}(K_a(t)U_a(t) - K_m(t)\omega(t)), \quad (2)$$

where $\omega(t)$ is the motor speed, $U_a(t)$ plays the role of the DC armature voltage,

$$U_a(t) = K_m(t)\omega(t) + R_a I_a(t), \quad (3)$$

$I_a(t)$ plays the role of the armature current, R_a of the armature resistance.

The quantities $K_a(t)$ and $K_m(t)$ are not constant as in DC motors, since they represent influence of the variable d,q voltages and currents performed by the motor controller. The equivalence between real AC quantities and fictitious DC counterparts $U_a(t)$, $I_a(t)$, $K_a(t)$, $K_m(t)$, and $R_a(t)$ is found by comparing (1) and (2–3).

2.1.2. Supercapacitor A simple equivalent circuit of a supercapacitor consists of a capacitor and a resistor in series (Sciarretta *et al.*, 2004). The Kirchhoff's voltage law yields

$$U_s(t) = \frac{Q(t)}{C} - R_s I_s(t), \quad I_s(t) = -\frac{dQ(t)}{dt}, \quad (4)$$

where $U_s(t)$ is the terminal voltage, $I_s(t)$ is the terminal current, R_s is the equivalent resistance, C is the capacitance, and $Q(t)$ is the charge.

2.1.3. DC/AC Link The electric power link between electric motor power P_a and supercapacitor power P_s is achieved with an inverter. We assume here that the motor torque is controlled by the voltage ratio $\lambda(t)$ of the inverter:

$$U_s(t) = \frac{1}{\lambda(t)}U_a(t), \quad I_s(t) = \lambda(t)I_a(t). \quad (5)$$

Because of internal physical constraints, it is not possible to control the electric motor with a continuous control variable $\lambda(t)$ when positive torque is requested. Instead, five discrete values of λ are available at each time t , as a function of the system operating conditions. This discrete controller permits to obtain five values of torque, depending on the supercapacitor voltage and the motor speed. The difference between minimum and maximum available torque does not exceed 2 Nm.

2.2 Dynamic model of the whole electric system

The physical causality representation of the whole electric system is sketched in Figure 2. The speed is an input variable, together with the controller λ . The torque is the output variable.

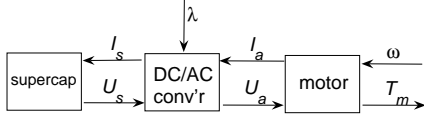


Fig. 2. Dynamic representation of the electric system

To obtain the dynamic dependency between torque and speed, we differentiate each term of (4), which leads to

$$\dot{U}_s(t) = -\frac{I_s(t)}{C} - R_s \dot{I}_s(t). \quad (6)$$

From (3) and (5) we obtain

$$I_s(t) = \lambda(t) \frac{\lambda(t)U_s(t) - K_a(t)\omega(t)}{R_a}. \quad (7)$$

From (6) and (7) we finally obtain

$$\dot{U}_s(t) = \frac{\lambda(t)}{1 + \lambda(t)^2 \frac{R_s}{R_a}} \left[-\frac{\lambda(t)U_s(t) - K_a(t)\omega(t)}{CR_a} + \frac{R_s}{R_a} K_a(t)\dot{\omega}(t) \right]. \quad (8)$$

The model given by (8) is validated against measurements taken on a dedicated test bench at Valeo. Figure 3 shows the transient behavior of the supercapacitor voltage resulting from a motor

speed step occurring in the first seconds of test. The experimental data are post-processed with a filter having a time constant of about 100 ms. Four speed levels are shown in the figure, ranging from 3000 rpm to 6000 rpm. Starting from an initial open-circuit value of 24 V, the supercapacitor voltage exhibits an abrupt drop of about 4 V, followed by a slower decrease. Consequently, the supercapacitor current (Figure 4) exhibits an initial step appearing as a smooth peak due to the low-pass filtering, followed by a slower decrease that would virtually end when the supercapacitor is completely discharged.

The comparison between experimental data and simulations of Figure 3 and 4 shows that the simplified approach of (8) is indeed able to represent the main dynamics of the system. The control parameters K_a and K_m have been parameterized as

$$K_a = \frac{K_{a0}}{\omega(t)}, \quad K_m = K_{m0} \frac{U_s(t)}{\omega(t)}. \quad (9)$$

The fitted values of the model parameters are listed in Table 1.

Table 1. Numerical values of the fitted model parameters

Parameter	Value
C	196 C
R_a	30.7 Ω
R_s	0.6 m Ω
K_{a0}	8
K_{m0}	125

The tests of Figures 3 and 4 were performed for a given setting of the discrete motor controller. In the simulations, that corresponds to a specific value λ_4 of the voltage ratio of the inverter. The torque curves calculated for all of the controller settings are shown in Figure 5. For the specific value λ_4 , the simulation results can be compared to experimental data.

2.3 Quasistatic model

A quasistatic counterpart of the model presented above is developed for the offline optimization. The causality representation of the electric system is sketched in figure 6.

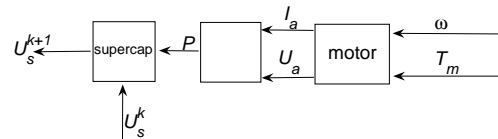


Fig. 6. Quasistatic representation of the electric system

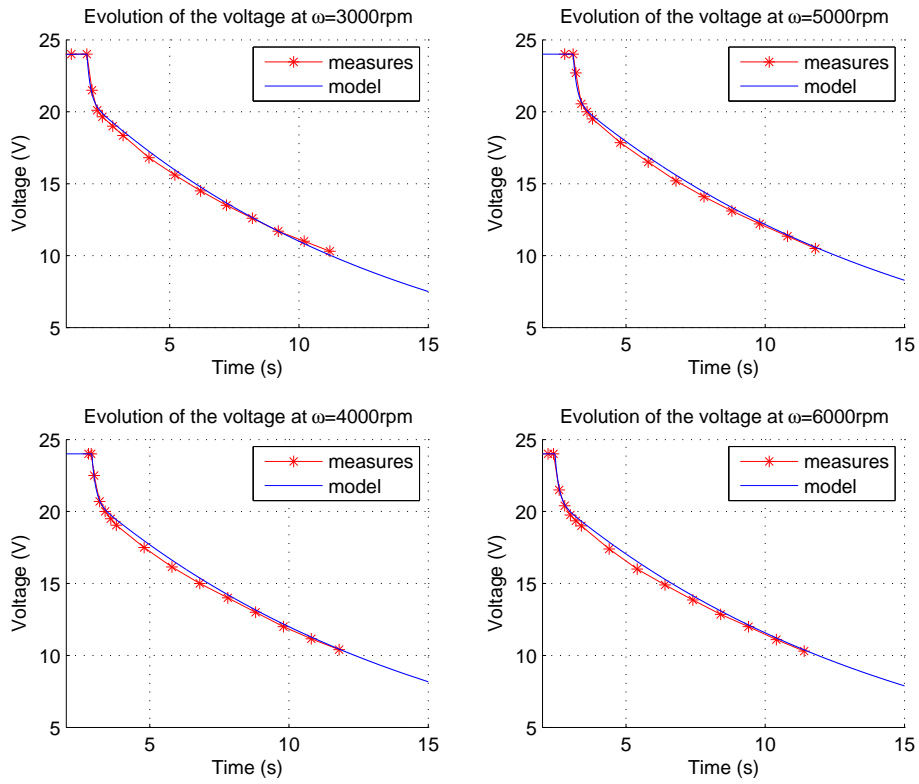


Fig. 3. Experimental data compared to model: evolution of the voltage $U_s(t)$

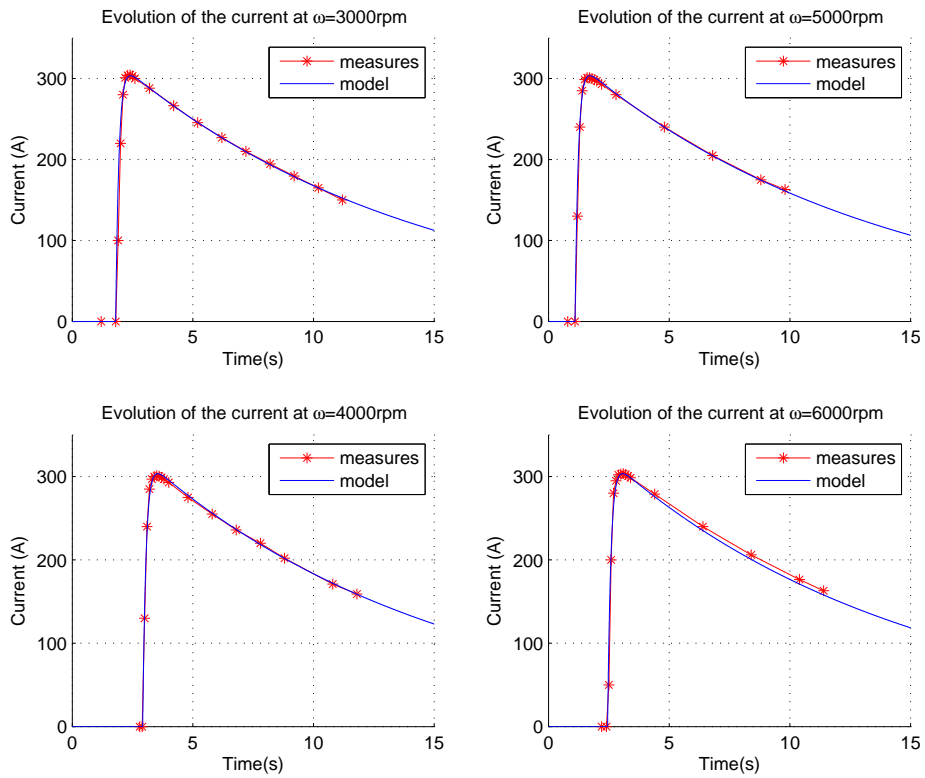


Fig. 4. Experimental data compared to model: evolution of the current $I_s(t)$

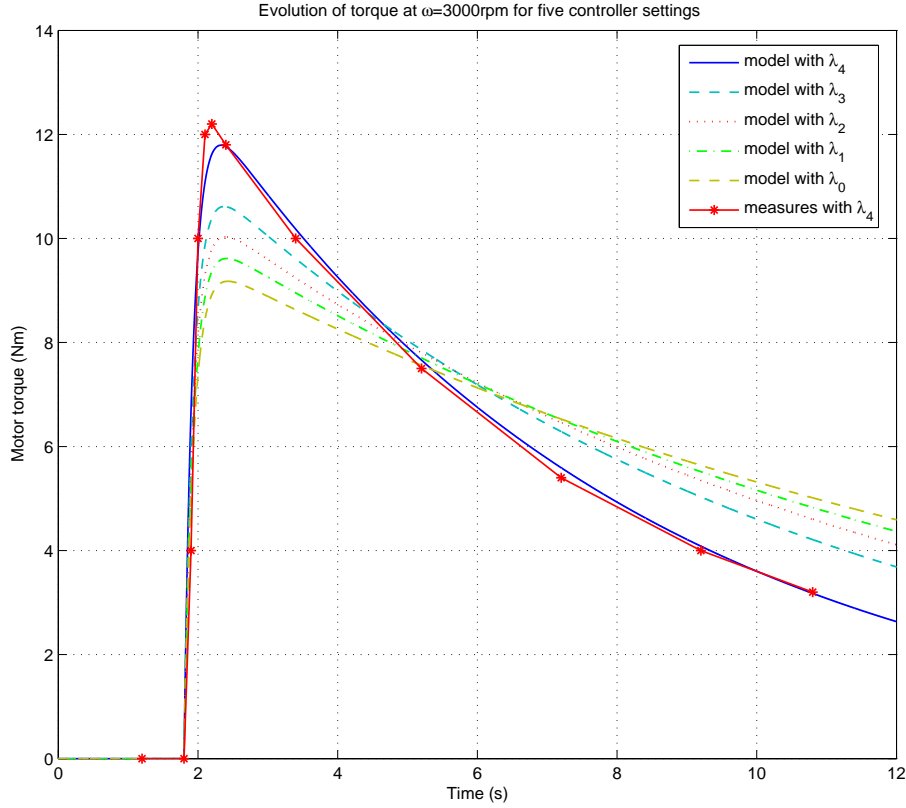


Fig. 5. Evolution of torque with different settings of the motor controller

From the motor speed $\omega(t)$ and torque $T_m(t)$ required, provided they are compatible with the physical limits of the motor, the armature voltage and current are computed with (2) and (3). The requested electric power is computed as

$$P(t) = U_a(t)I_a(t), \quad (10)$$

and, assuming no conversion losses as in (5), is also $P(t) = U_s(t)I_s(t)$.

From (4) and (10) we obtain a differential equation for $U_s(t)$ as a function of $P(t)$,

$$\left(1 - \frac{R_s P(t)}{U_s^2(t)}\right) \frac{dU_s^2(t)}{dt} = -2\frac{P(t)}{C} - 2R_s \dot{P}(t). \quad (11)$$

Using numerical integration methods, this equation is integrated at any time using the value of U_s at the previous time step

$$U_{k+1}^2 = -\frac{2P_k \bar{U}_k^2 \Delta t}{C(\bar{U}_k^2 - R_s P_k)} + U_k^2, \quad (12)$$

with:

- Δt : constant time step,
- U_k, U_{k+1} : supercapacitor voltage at time step k and $k+1$,
- \bar{U}_k : average voltage during time interval $[k, k+1]$,

- P_k : electric power during time interval $[k, k+1]$.

In (12), we have neglected the term proportional to \dot{P} of (11) since $R_s C \ll \Delta t$.

The consequent value of λ to obtain the requested torque T_m is calculated using

$$I_{sk} = P_k / \bar{U}_k, \quad (13)$$

then, with (5):

$$\lambda_k = I_{sk} / I_{ak}. \quad (14)$$

3. DYNAMIC PROGRAMMING OPTIMIZATION

3.1 Optimal Control Problem

The optimal control problem under study consists in minimizing the fuel consumption of the vehicle along a prescribed driving cycle, while providing charge sustenance to the supercapacitor, and taking into account physical limits of the supercapacitor, the engine, and the electric motor.

We define the control variable $u(t)$ which represents the split factor of the requested torque T_{rq} , between the engine torque T_e and the motor torque T_m :

$$\begin{cases} T_{rq}(t) = T_e(t) + \rho T_m(t) \\ T_e(t) = u(t)T_{rq}(t) \end{cases}, \quad (15)$$

where ρ corresponds to the ratio between engine speed and electric motor speed.

The only relevant dynamics considered is that of supercapacitor voltage, called $U(t)$ in the following, which follows from (11)

$$\dot{U}(t) = f(U(t), u(t), t). \quad (16)$$

The resulting optimization problem is then the following :

$$\begin{cases} \min_{u \in W(t)} \left\{ J(u) = \int_0^T L(u(t), t) dt + g(U(T), T) \right\} \\ \text{subject to : } \dot{U}(t) = f(U(t), u(t), t), \quad U(0) = U_0 \end{cases} \quad (17)$$

where T is the final time of the drive cycle, $L(u(t), t)$ is the fuel consumption rate, computed from the data displayed in Figure 1, $g(U(T), T)$ is a term that penalizes any deviation of the final voltage from the initial voltage.

In addition to the latter ‘‘soft’’ constraint over the final state, the problem (17) is also subjected to the following inequality constraints, leading to the feasible control space $W(t)$:

- the engine can only produce a positive torque, which is limited to a maximum torque that depends on engine speed $\omega_{rq}(t)$, leading to the control constraints

$$0 \leq u(t)T_{rq}(t) \leq T_e^{max}(\omega_{rq}(t)), \quad (18)$$

- the electric motor torque is limited between a maximum torque and a minimum torque during generating operation, leading to the control constraints

$$\begin{aligned} \rho T_m^{min}(\omega(t)) &\leq (1 - u(t))T_{rq}(t) \\ &\leq \rho T_m^{max}(\omega(t)), \end{aligned} \quad (19)$$

- the motor controller can only be set to one over five discrete values, thus

$$\lambda(t) \in (\lambda_i)_{i \in [0,4]}, \quad (20)$$

as already discussed; that also leads to corresponding control constraints.

The state variable is also subjected to inequality constraints, deriving from physical limits of the supercapacitor and of the motor,

$$U_{min} \leq U(t) \leq U_{max}. \quad (21)$$

The values of U_{min} and U_{max} are set to 16 V and 24 V respectively.

3.2 DP Optimization algorithm

The Dynamic Programming method (DP) is classically used to solve the problem (17) ((Wu *et al.*, 2002), (Scordia, 2004)). It relies on the principle of optimality or Bellman principle. First, the optimal control problem (17) is discretized in time

$$\begin{cases} \min_{u_k \in W_k} J(u) := \sum_{k=0}^{N-1} L_k(u_k) + g(U_N) \\ \text{subject to : } U_{k+1} = f_k(U_k, u_k), \quad U(0) = U_0 \\ U_{min} \leq U_k \leq U_{max} \end{cases} \quad (22)$$

where $L_k(u_k)$ is the fuel consumption over the time interval $[k, k + 1]$, U_k is the voltage of the supercapacitor at time k , f_k is the function (16) at time k , and $g(U_N) = \beta(U_N - U_0)^2$ is the penalization term (β is a constant to be chosen), N is the final time, W_k the feasible domain for u_k with respect to constraints (18), (19), and (20).

From Bellman principle, the cost-to-go function $V_k(x_k)$ at the time step k , $0 \leq k \leq N - 1$, is expressed as

$$V_k(U_k) = \min_{u_k \in W_k} (L_k(u_k) + V_{k+1}(f_k(U_k, u_k))). \quad (23)$$

At time N , the cost-to-go is $V_N(x_N) = g(x_N)$.

This optimization problem is solved backward from final time step to initial time step using a discretization of function V in the control space and in the state space.

3.2.1. Model implementation As to control the electric system, both quasistatic and dynamic models are used. First, from a requested torque T_{rq} , the quasistatic model (10)–(14) is used to calculate the corresponding necessary value of λ , namely λ_{rq} . Then, only the control set u_{adm} that corresponds to the set λ_{adm} as

$$\lambda_{adm} = \{\lambda \mid \lambda \in (\lambda_i)_{i \in [0,4]}, \lambda \leq \lambda_{rq}\} \quad (24)$$

is tested.

A standard time step used in our examples is 1 s. The solving algorithm used is that of (Guilbaud, 2002) to which we refer for some theoretical results on the convergence and error estimations.

3.3 Optimization Results

The optimal system trajectories are calculated for the Urban Artemis cycle, shown in Figure 7. The figure also shows the optimal trajectory of motor torque, which exhibits a somehow intuitive behavior. The motor is used to assist the engine during accelerations, and as a generator during

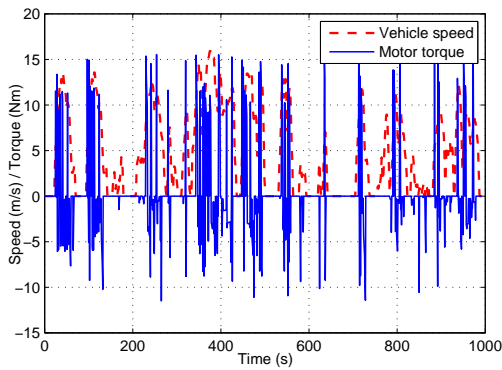


Fig. 7. Vehicle speed on Artemis Cycle / Optimal trajectory of motor torque

decelerations and during low-speed, low-torque phases.

The optimal voltage trajectory of the supercapacitor is presented in Figure 8. The figure clearly shows that, since the efficiency of the electric powertrain is higher at high voltage, the electric motor is used mostly between 20 V and 24 V.

The fuel consumption gain between pure engine mode and optimal hybrid mode is about 11%. Clearly, the system is not designed to achieve substantial improvements in fuel economy with respect to the conventional architecture, but rather to improve its performance, e.g., in terms of acceleration responses at low speed.

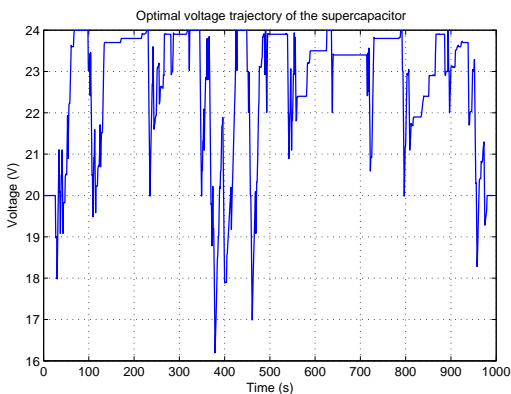


Fig. 8. Optimal voltage trajectory on Artemis cycle (minimal and maximal bounds on voltage: 16V and 24V)

4. REAL-TIME FEEDBACK CONTROL

In this section, suboptimal control law is derived from the optimization results.

Figure 9 shows the optimal values of the electric motor torque as a function of requested torque and speed. When negative torques are required, i.e., during regenerative braking, the whole torque available is used to recharge the supercapacitor.

The factor “2” between negative electric motor torque and negative requested torque comes from the speed ratio between engine and electric motor ($\rho = 1.96$).

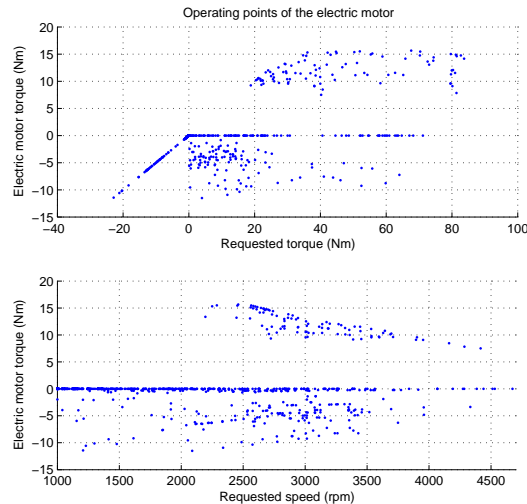


Fig. 9. Optimal electric motor torque T_m^o as a function of torque and speed requests, calculated with DP for the Artemis cycle.

For positive requested torque, the following behavior can be observed:

- the electric machine is only used as a motor above 2200 rpm (engine speed). Below this speed, the electric machine can be used to recharge the supercapacitor,
- the electric machine is only used as a motor when the requested torque is higher than 20 Nm, while it is used in the recharging mode in all the requested torque range, with a predominance of low requested torques (0 to 20 Nm).

An intuitive controller can be derived from these considerations, based on operating domains as a function of speed and torque requests, as shown in Figure 10.

In the boosting operating domain (positive motor torque area), the motor torque is subjected to the constraint (20). Figure 11 shows the optimal values of the discrete controller setting $\lambda(t)$ along the Artemis Cycle. Clearly, the optimal choice consists in selecting always the minimum admissible value λ_0 , which corresponds to the minimum admissible motor torque. It can be proven that this choice maximizes the efficiency of the electric subsystem.

In the regenerating operating domain (negative motor torque area) of Figure 10, the controller setting λ can be varied continuously, meaning that the recharging torque can have every value below the physical limit $-T_m^{min}$.

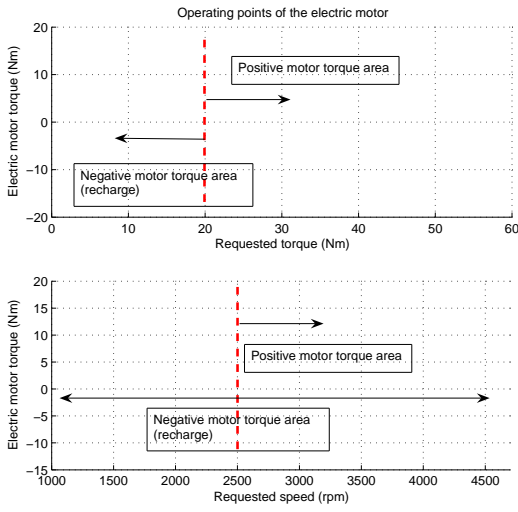


Fig. 10. Operating domains of the electric motor as a function of torque and speed requests

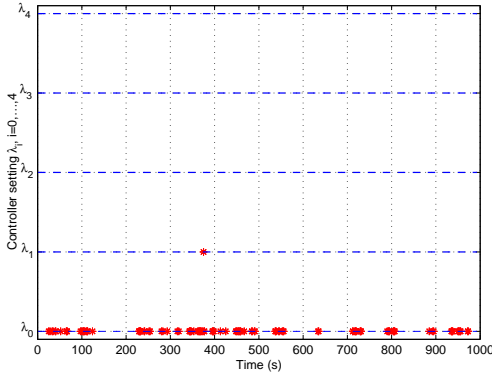


Fig. 11. Optimized discrete control $\lambda_i, i = 0, \dots, 4$ Searching for a simple heuristic rule to represent the optimal motor behavior, it seems rather intuitive to compare the optimal regenerating torque of Figure 9, T_m^o with the torque values that maximize the global efficiency of the system, \hat{T}_m . When the engine recharges the supercapacitor through the electric machine, the global efficiency is calculated as

$$\eta_{charge} = \frac{\frac{1}{2}CU_s\Delta U_s}{H_i\Delta L\Delta t}, \quad (25)$$

where ΔU_s the variation of the supercapacitor voltage for the time step Δt and ΔL is the additional fuel consumption rate that is used to recharge the supercapacitor.

A comparison between T_m^o and \hat{T}_m is shown in Figure 12 for the Artemis cycle. Clearly, the two data sets are very different. Consequently, the optimal motor behavior during regeneration phases cannot be simply described by a rule based on (25). The reason is that the optimal motor torque when recharging the supercapacitor does not depend on local conditions only, but it is a function of the optimal motor torque during

boosting phases, as well as of the state boundaries and final state constraint.

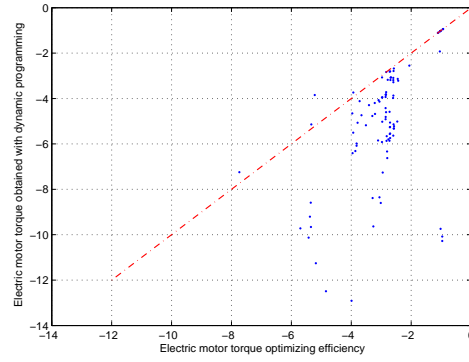


Fig. 12. Relation between calculated electric torque

Noncausal solutions of the optimal control problem (17) may lead to approximate, suboptimal controllers that perform better than heuristic feedback controllers, like the one described in this section, in representing the optimal behavior of the system.

5. CONCLUSIONS

In this paper, we have proposed a dynamic model of the electric system used in a mild hybrid vehicle. The model is based on physical equations of a DC electric motor, a supercapacitor, and an inverter. The model parameters have been successfully fitted to experimental data in order to simulate accurately the behavior of the electric system.

This dynamic model has been used in a Dynamic Programming algorithm to minimize the fuel consumption, taking into account the main physical constraints of the system (especially the discrete control settings). The optimal trajectory leads to an interesting gain in fuel consumption (9%) despite the reduced size of the electric motor and capacity of the supercapacitor.

From the optimization results on the Artemis cycle operating domains for the different electric motor modes (assist or recharge) were derived. For each domain a heuristic control law adapted to the electric motor mode was defined. Although the heuristics is able to represent a good approximation of the optimal switching between operating modes, it appeared to be a too simplified approach to calculate the optimal motor torque trajectories.

Future work will therefore include the synthesis of a noncausal controller based on an appropriate, although approximate, solution of the optimal control problem.

REFERENCES

- Dabadie, J.C., P. Menegazzi, R. Trigui and B. Jeanneret (2005). A new tool for advanced vehicle simulations. *ICE - 7th International Conference on Engine for Automotive, Capri, Italy*.
- Delprat, S. (2002). Evaluation de stratégies de commande pour véhicules hybrides parallèles. PhD thesis. Université de Valenciennes et du Hainaut-Cambresis.
- Guilbaud, T. (2002). Méthodes numériques pour la commande optimale. PhD thesis. Université de Paris VI.
- Sciarretta, A., L. Guzzella and M. Back (2004). A real-time optimal control strategy for parallel hybrid vehicles with on-board estimation of the control parameters. *Proceedings of IFAC Symposium on Advances in Automotive Control AAC04* pp. 502–507.
- Scordia, J. (2004). Approche systématique de l’optimisation du dimensionnement et de l’élaboration de lois de gestion d’énergie de véhicules hybrides. PhD thesis. Université Henri Poincaré - Nancy 1.
- Tilagone, R. and S. Venturi (2004). Development of natural gas demonstrator based on an urban vehicle with a down-sized turbocharged engine. *Oil and Gas Science and Technology* **59**(6), 581–591.
- Wu, B., C-C. Lin, Z. Filipi, H. Peng and D. Assanis (2002). Optimization of power management strategies for a hydraulic hybrid medium truck. *Proceeding of the 2002 Advanced Vehicle Control Conference, Hiroshima, Japan*.

ACKNOWLEDGMENTS

We would like to thank Paolo Tona and Pierre Rouchon for helpful discussions and advice at various stages of the elaboration of this work. We acknowledge Quang Huy Tran for his advice on numerical methods. We thank Sylvain Delion from Valeo for providing data and for his advice about the model.